Dynamics of visual object coding within and across the hemispheres: Objects in the periphery

Amanda K. Robinson[1,2*], Tijl Grootswagers[3], Sophia M. Shatek[2], Marlene Behrmann[4], Thomas A. Carlson[2]

[1] School of Psychology, The University of Queensland, Brisbane, Australia.
[2] School of Psychology, University of Sydney, Sydney, Australia.
[3] The MARCS Institute for Brain, Behaviour and Development, Western Sydney University, Sydney, Australia.
[4] Department of Psychology, Carnegie Mellon University and University of Pittsburgh, USA.
[*] Corresponding author: amanda.robinson@uqconnect.edu.au

Abstract

The human brain continuously integrates information across its two hemispheres to construct a coherent representation of the perceptual world. Characterising how visual information is represented in each hemisphere over time is crucial for understanding how hemispheric transfer contributes to perception. Here, we investigated information processing within each hemisphere over time and the degree to which it is distinct or duplicated across hemispheres. We presented participants with object images lateralised to the left or right visual fields while measuring their brain activity with electroencephalography (EEG). Stimulus coding was more robust and emerged earlier in the contralateral than the ipsilateral hemisphere. Presentation of two stimuli, one to each hemifield, reduced the fidelity of representations in both hemispheres relative to one stimulus alone, signifying hemispheric interference. Finally, we found that processing within the contralateral, but not ipsilateral, hemisphere was biased to image-related over concept-related information. Together, these results suggest that hemispheric transfer operates to filter irrelevant information and efficiently prioritise processing of meaning.

Introduction

The human brain has two distinct but connected hemispheres that must communicate and coordinate to yield unitary visual perception. Due to the contralateral arrangement of the visual system, stimuli presented to one hemifield are initially processed in the opposite hemisphere. Yet, from this hemisphere-distinct processing a single coherent percept of the visual world emerges, highlighting the importance of hemispheric integration. The nature of hemispheric processing has fascinated cognitive neuroscientists for decades. For example, studies using split-brain patients, who had the corpus callosum surgically severed, have shown that the left and right hemispheres can have different perceptual experiences and responses to the same stimulus (*1*, *2*). The mechanisms underlying hemispheric transfer are complex, involving communication between brain regions at different levels of processing, but understanding how neural processing results in perception requires a better understanding of information processing within and across hemispheres.

The left and right hemispheres of the brain are largely homologous in terms of structure and function. The strength in this duplication, or redundancy, can be borne out in behaviour; for example, interhemispheric cooperation can improve performance on highly complex tasks (*3*, *4*). Neurally, interhemispheric communication is facilitated by a number of anatomical connections between the left and right hemispheres, including the corpus callosum, posterior commissure, and anterior commissure (*5*–*7*). These connections allow the two hemispheres to share information and coordinate their activities. For visual perception, the integration of information across the hemispheres is crucial, yet is not as well characterised as other aspects of visual processing. The hierarchical nature of visual processing has been well-studied; across the swath of visual cortex, there is a hierarchical flow of features, starting with sensitivity to low-level features such as straight edges coded in primary visual cortex, through successive stages to higher level categorical features associated with specific patterns (e.g. words or faces) coded in ventral temporal cortex (*8*, *9*). Models of the visual system, however, typically do not consider the interplay between

the two hemispheres, despite their joint involvement in perception. In this paper, we map the dynamics of information coding within each hemisphere and the sharing of this information across hemispheres.

Neural recordings have shed light on the computations that underlie hemispheric processing. Studies using electroencephalography (EEG) in humans have shown earlier and stronger evoked responses over the scalp contralateral to stimulus presentation relative to the ipsilateral side, consistent with the trajectory of fibres from the eyes to the contralateral hemisphere (*10*–*12*). Inter-hemispheric transfer time calculated from event-related potentials in occipital brain regions have been observed between 13ms and 26ms (*10*, *12*, *13*), varying by stimulus location and intensity (*14*, *15*). The inferred but untested implication is that the contralateral hemisphere initially registers the sensory information, and then propagates a subset of this information to the ipsilateral hemisphere. Yet, strength of neural activation is not necessarily correlated with strength of information coding (*16*). A pertinent question, then, and the focus of this paper is how the representations derived in the contralateral and ipsilateral hemispheres differ.

Studying hemispheric information has proven difficult in humans due to traditional analytic methods of neural data that obscure subtle neural patterns of activity. With the advent of multivariate pattern analyses (MVPA), or neural "decoding", however, we can study *what* is represented in the brain using non-invasive neural recordings in humans (*17*). Combined with high temporal resolution neuroimaging methods such as electroencephalography (EEG), MVPA can elucidate the time course and fidelity of stimulus information within neural patterns of activity. Time-resolved neural decoding methods have shown that visual information is represented quickly in the brain, occurring in less than 100ms from stimulus onset (*18*, *19*). Notwithstanding this rapid time course, EEG has sufficient resolution to detect high spatial frequency neural activity early in the course of signal propagation (*20*), making it possible to separate signals from the left and right hemispheres and permitting opportunities to study dynamics of information within each hemisphere.

In this paper, we use EEG and multivariate analyses to investigate the representation of visual information within each hemisphere and the similarities across hemispheres over time. We employed a rapid serial visual presentation (RSVP) paradigm with visual stimuli presented to the left and right hemifields while neural activity was measured using EEG (Figure 1). The goals of this study were threefold. First, we assessed how the contralateral and ipsilateral hemispheres process visual signals from the periphery (projected just to one hemisphere initially) over time. Second, we presented stimuli to the left and right hemifields simultaneously to understand how processing changes when different signals project to the two hemispheres, with the expectation that there might be interference in the representations. Finally, to understand the content of hemispheric information, we assessed how the neural representations per hemisphere compare to similarity judgements on independent perceptual and conceptual tasks. We found clear contralateral dominance in the strength of visual coding, as expected. Further, we found reduction in information when two different stimuli were shown, one to each hemifield, suggesting that there may be interference or competition for representation between contralateral and (propagated) ipsilateral information. With respect to behaviour, we found that the contralateral hemisphere contains more information relevant to perceptual than conceptual judgements, but that this perceptual bias is largely missing in the ipsilateral hemisphere. This finding provocatively indicates that hemispheric transfer might efficiently prioritise meaning, rather than image statistics. These results yield great insights into hemispheric processing, the complex interplay between the two hemispheres and how they cooperate to create a unified representation of the visual world.

Figure 1. Experimental design.

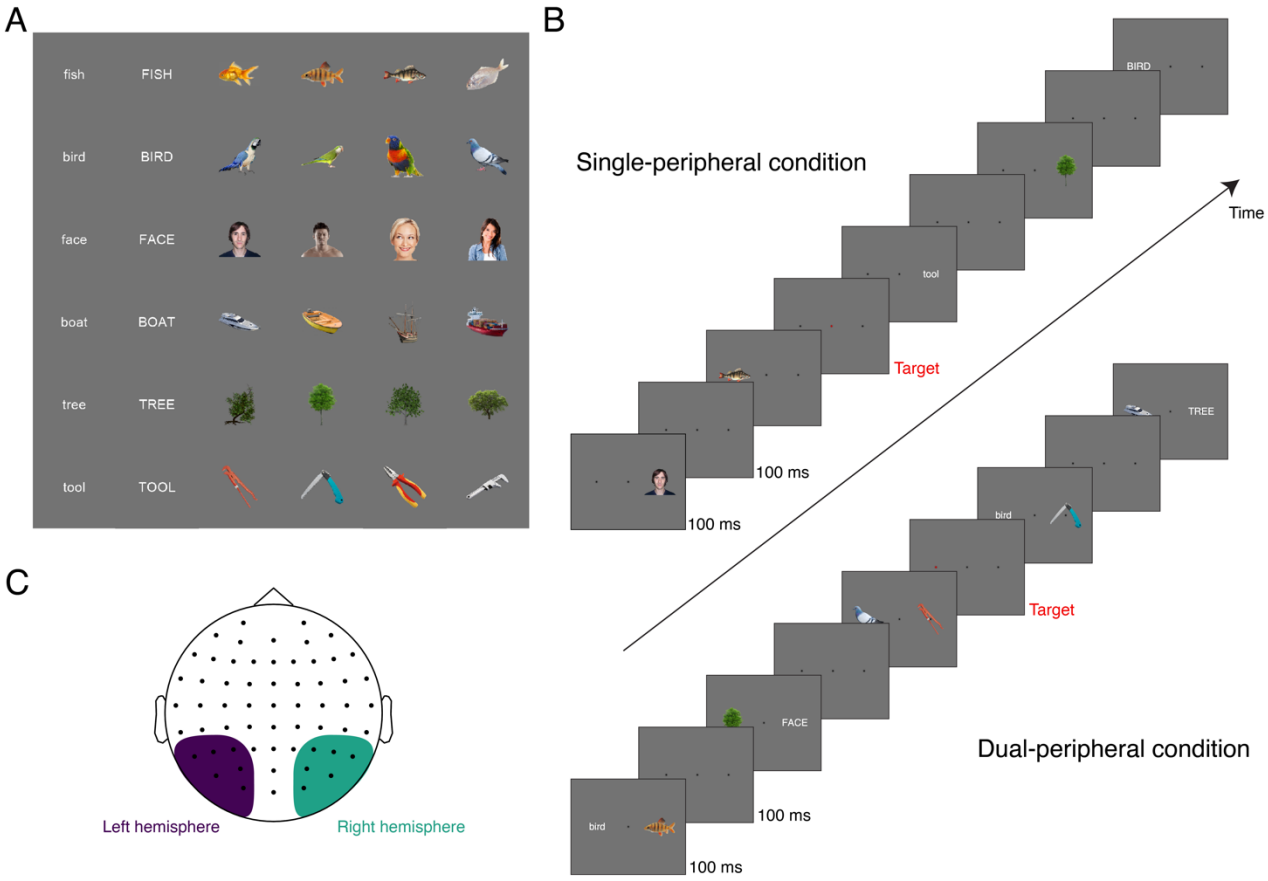

Note. A) Stimuli were 36 images of objects and matching word labels for six different object categories. B) Example sequence timeline for single-peripheral and dual-peripheral conditions. C) Electrode clusters for left hemisphere and right hemisphere analyses.

Results

Neural dynamics of stimulus representations: single-peripheral condition

To investigate hemispheric dynamics when processing was biased to one hemisphere, we assessed the neural representations of stimuli shown peripherally to the contralateral and ipsilateral visual fields (Figure 1B; top). We used neural decoding methods applied to the event-related EEG data to assess stimulus-specific representations per hemifield (left/right) and hemisphere (left/right).

Decoding was performed separately using clusters of electrodes measuring from the left and right hemispheres over time (Figure 1C). Stimulus information coded within each hemisphere, as indexed by mean pairwise decoding accuracy for the 36 stimuli, showed

clear contralateral dominance (Figure 2A,B). In the left hemisphere, right visual field (RVF) stimuli showed higher decoding and earlier onset (peak = 53.39%, onset = 79ms) than left visual field (LVF) stimuli (peak = 51.68%, onset = 96ms). Similarly, in the right hemisphere, the contralateral (LVF) stimuli showed higher decoding and earlier onsets (peak = 54.98%, onset = 78ms) than RVF stimuli (peak = 52.53%, onset = 91ms; see Table 1). Interestingly, representations in the right hemisphere were stronger than those in the left hemisphere for both contralateral and ipsilateral stimuli (Figure 2C), consistent with previous reports (*21*). Notably, this right-hemispheric dominance was not driven by the faces in the stimulus set; the 18 non-face objects also produced stronger right hemisphere representations when analysed separately (see Supplementary Material). Overall, for single stimuli presented to a hemifield, decoding peaked earlier for the contralateral stimuli than the ipsilateral stimuli, providing further support for differing dynamics in each hemisphere and a contralateral precedence in the visual system. Next, we turned to how the dynamics of representation varied when there were competing visual inputs from the two hemifields.

Figure 2. Peripheral stimulus representations in the left and right hemispheres (single-peripheral condition)

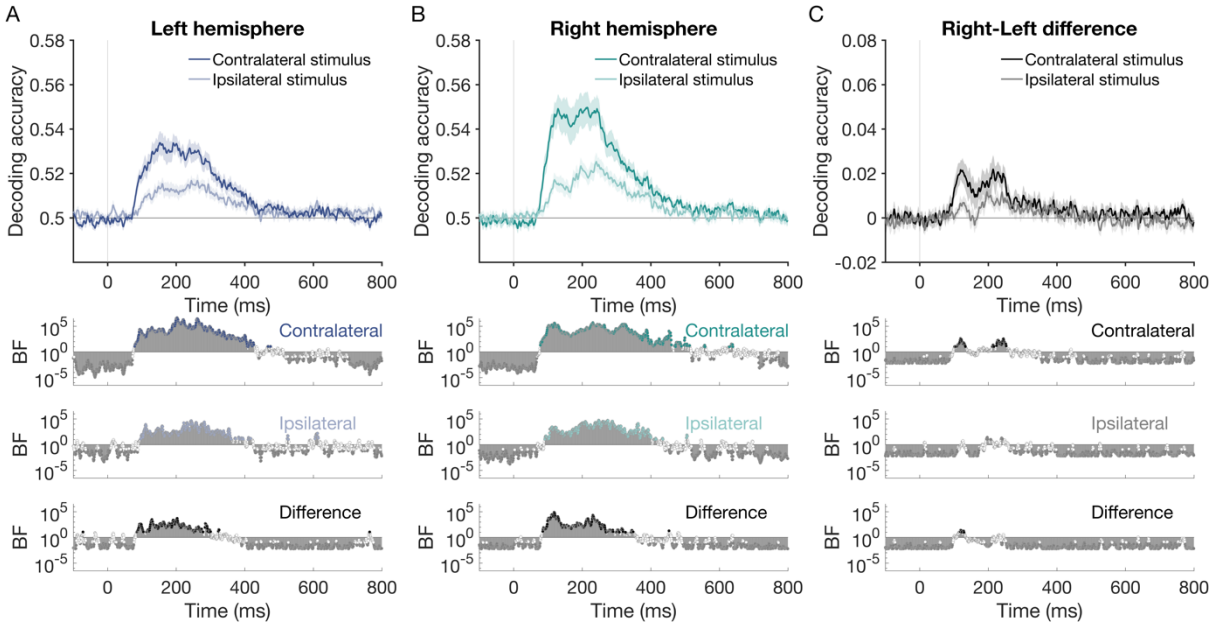

Note. Neural representations for stimuli in the single peripheral condition across time (1 ms resolution), as indexed by mean decoding accuracy of pairs of experimental stimuli. Accuracy of decoding is plotted separately for stimuli appearing in the contralateral and ipsilateral visual fields. A) Decoding using cluster of electrodes over the left hemisphere. B) Decoding using cluster of electrodes over the right hemisphere. C)

Difference between right and left hemisphere decoding accuracy. Shaded lines indicate standard error of the mean. Contralateral representations were stronger, with earlier peaks and onsets than ipsilateral representations. Right hemisphere representations were stronger than the left for contralateral stimulus presentations. Bottom plots show Bayes Factors which indicate the evidence for above chance decoding per condition or non-zero differences between conditions.

Neural dynamics of stimulus representations: dual-peripheral condition

We were interested in how representational dynamics varied according to the contralateral and ipsilateral side when two stimuli were presented simultaneously: one to the left visual field and one to the right visual field (Figure 3). Given the ubiquitous nature of hemispheric transfer, we expected that the fidelity of stimulus information might be reduced when there are competing inputs to the two hemispheres. For this dual-peripheral condition, decoding was performed for each stimulus separately but, now, in the context of a second stimulus in the other field. Again, as above, there was clear contralateral dominance in both the left and right hemispheres (Figure 3A,B). In the left hemisphere, the RVF stimuli showed higher decoding and earlier onset (peak = 53.13%, onset = 69ms) than LVF stimuli (peak = 50.93%, onset = 99ms). Echoing these results, in the right hemisphere the contralateral (LVF) stimuli showed higher decoding and earlier onsets (peak = 54.49%, onset = 78ms) than RVF stimuli (peak = 51.27%, onset = 85ms). Right hemisphere superiority was reliable for contralateral but not ipsilateral representations (Figure 3C). Together, these results show that even when there is competing information from the two hemifields, information about each stimulus is processed by both hemispheres of the brain at the same time. Whether these dynamics were similar between the single- and dual-peripheral conditions was tested next.

Figure 3. Peripheral stimulus representations in the left and right hemispheres (dual-peripheral condition).

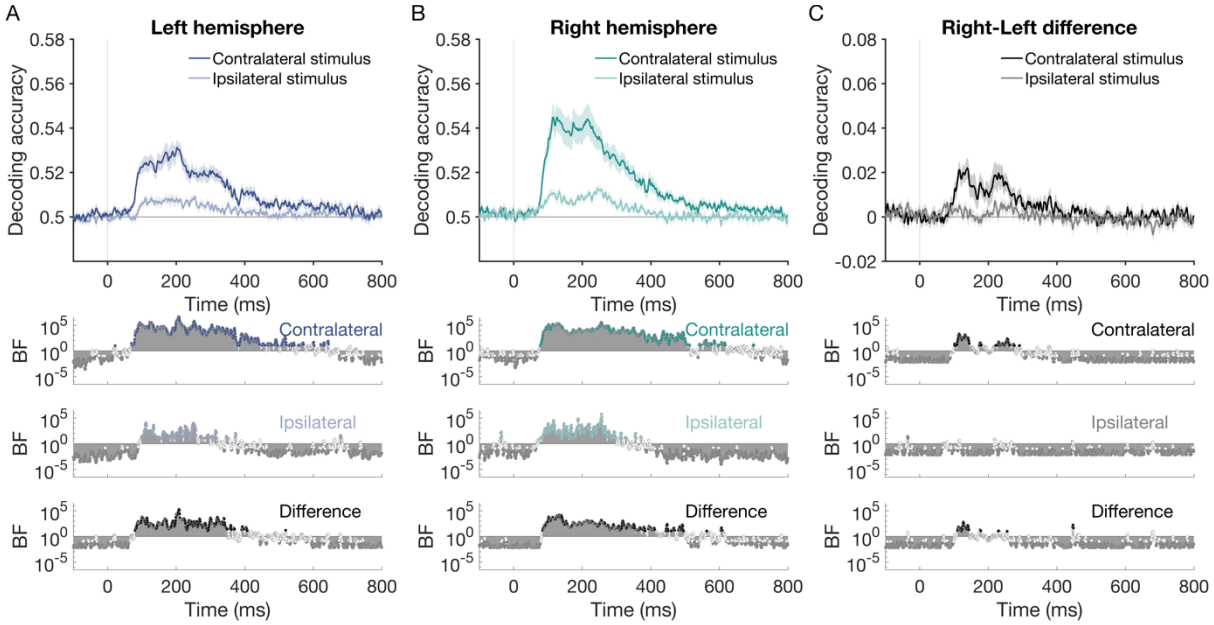

Note. Neural representations when two stimuli are presented to different hemispheres, as indexed by mean pairwise decoding accuracy. Accuracy is plotted separately for stimuli appearing in the contralateral and ipsilateral visual fields. A) Decoding using cluster of electrodes over the left hemisphere. B) Decoding using cluster of electrodes over the right hemisphere. C) Difference between right and left hemisphere decoding. Shaded lines represent standard error of the mean. Onsets and peaks are marked above the x-axes. Representations for the contralateral stimuli were stronger, with earlier peaks and onsets than for ipsilateral stimuli. Right hemisphere representations were stronger than the left for contralateral stimuli. Bottom plots show Bayes Factors which indicate the evidence for above chance decoding per condition or non-zero differences between conditions.

Comparison of single and dual-peripheral presentation

To assess whether the addition of a second stimulus in the dual-peripheral condition interfered with the fidelity of stimulus representations, we compared the timing and strength of decoding in the single- and dual-peripheral conditions. Inspection of decoding onset time revealed earlier onsets for contralateral than ipsilateral stimuli, with contralateral decoding beginning before 80ms and ipsilateral decoding tending to begin after 90ms, regardless of which hemisphere or condition was being assessed (Table 1). Thus, the initial stage of stimulus processing was not influenced by clutter in the display.

Table 1. Onset time (with 95% confidence intervals in brackets) and peak decoding accuracy for single- and dual-peripheral conditions.

		Onset time		Peak decoding accuracy	
		Left hemisphere	Right hemisphere	Left hemisphere	Right hemisphere
Single-peripheral	Contralateral	79 [77-81]	78 [77-79]	53.39%	54.98%
	Ipsilateral	96 [91-104]	91 [90-104]	51.68%	52.53%
Dual-peripheral	Contralateral	69 [68-78]	78 [76-82]	53.13%	54.49%
	Ipsilateral	99 [97-105]	85 [79-87]	50.93%	51.27%

Note. Onsets and peaks according to condition (single-/dual-peripheral), hemisphere and whether the stimulus was contralateral or ipsilateral relative to hemisphere. Onsets were calculated as the time of the first time Bayes Factors were above 10 for 10 ms consecutively. Confidence intervals were calculated using jackknifing to subsample participants (leave-two-participants-out; 190 unique permutations) to yield a distribution of onsets.

However, there was a decrease in stimulus-related information in the brain in the dual-peripheral relative to the single-peripheral condition (Figure 4). To compare the representations encoded by the brain between conditions, we assessed decoding accuracy in each condition for contralateral and ipsilateral stimuli, collapsed across the left and right hemispheres. For both contralateral and ipsilateral combinations, stimulus representations were more robust for the single-peripheral than the dual-peripheral condition, indicating that a stimulus presented in the other visual field decreased the fidelity of stimulus representations.

Figure 4. Decoding accuracy for peripheral stimuli when presented alone (single) or with another stimulus (dual).

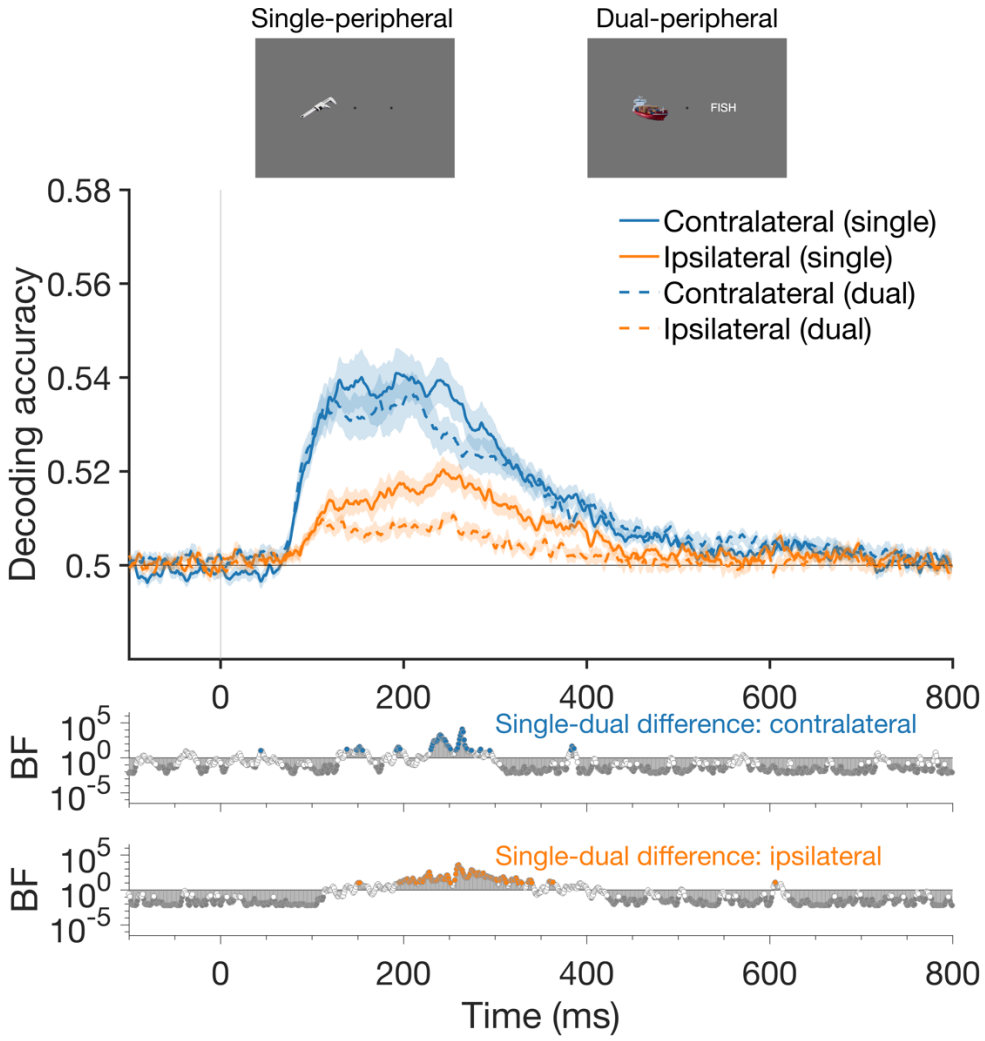

Note. Decoding accuracy is plotted according to whether stimuli were contralateral or ipsilateral relative to the electrode cluster. These results are collapsed across the left and right hemispheres. Information was stronger in the single-peripheral condition than the dual-peripheral condition (see BFs for difference), for both contralateral and ipsilateral stimuli. Shaded lines represent standard error of the mean. Bottom plots show Bayes Factors indicating the evidence for non-zero differences between single and dual conditions.

Representational similarity analyses: comparison across hemispheres

We were next interested in the structure of representations in the two hemispheres of the brain. The hypothesis was that stimulus coding in the ipsilateral hemisphere should reflect the same representations as the contralateral hemisphere, but following a delay approximating interhemispheric transfer time. To investigate the relationship between representations in the two hemispheres, we used representational similarity analyses (RSA)

(*22*), which abstracts away from specific activity patterns (e.g., from EEG electrodes over the left hemisphere) to the relationships between different stimulus representations.

For each presentation condition (single-peripheral, dual-peripheral), stimulus visual field (LVF/RVF), time point and participant, we constructed neural representational dissimilarity matrices (RDMs) to quantify the dissimilarity in the representations of all 36 stimuli (i.e., in a 36 × 36 matrix with 630 unique values). The RDMs from the left and right hemispheres were then correlated for all possible time points (Figure 5A). These analyses were performed in a split-half manner, where correlations were always calculated across separate experimental sequences. Correlations between contralateral and ipsilateral hemispheres were assessed by collapsing across relevant visual field and left/right hemispheres. We found evidence for shared representations across the contralateral and ipsilateral hemispheres, particularly between 100-300ms after stimulus onset (Figure 5B). These correlations were more reliable for the single-peripheral condition than the dual-peripheral condition. This suggests that information that is transferred from the contralateral to ipsilateral hemisphere maintains stimulus-specific structure, but that transfer is reduced in the case of competing information (as in the dual-peripheral condition).

To assess the timing of information sharing, we assessed the number of time points with reliable correlations (BF>3) as a function of time for the contralateral and ipsilateral hemispheres. As expected, times were earlier for the contralateral than ipsilateral hemisphere (Figure 5C). A quantification of the time delay (ipsilateral-contralateral difference) for each reliable correlation revealed a consistent delay of shared information from the contralateral to ipsilateral hemisphere that was most commonly between 15-30ms (Figure 5D).

Figure 5. Shared structure of representations across the hemispheres.

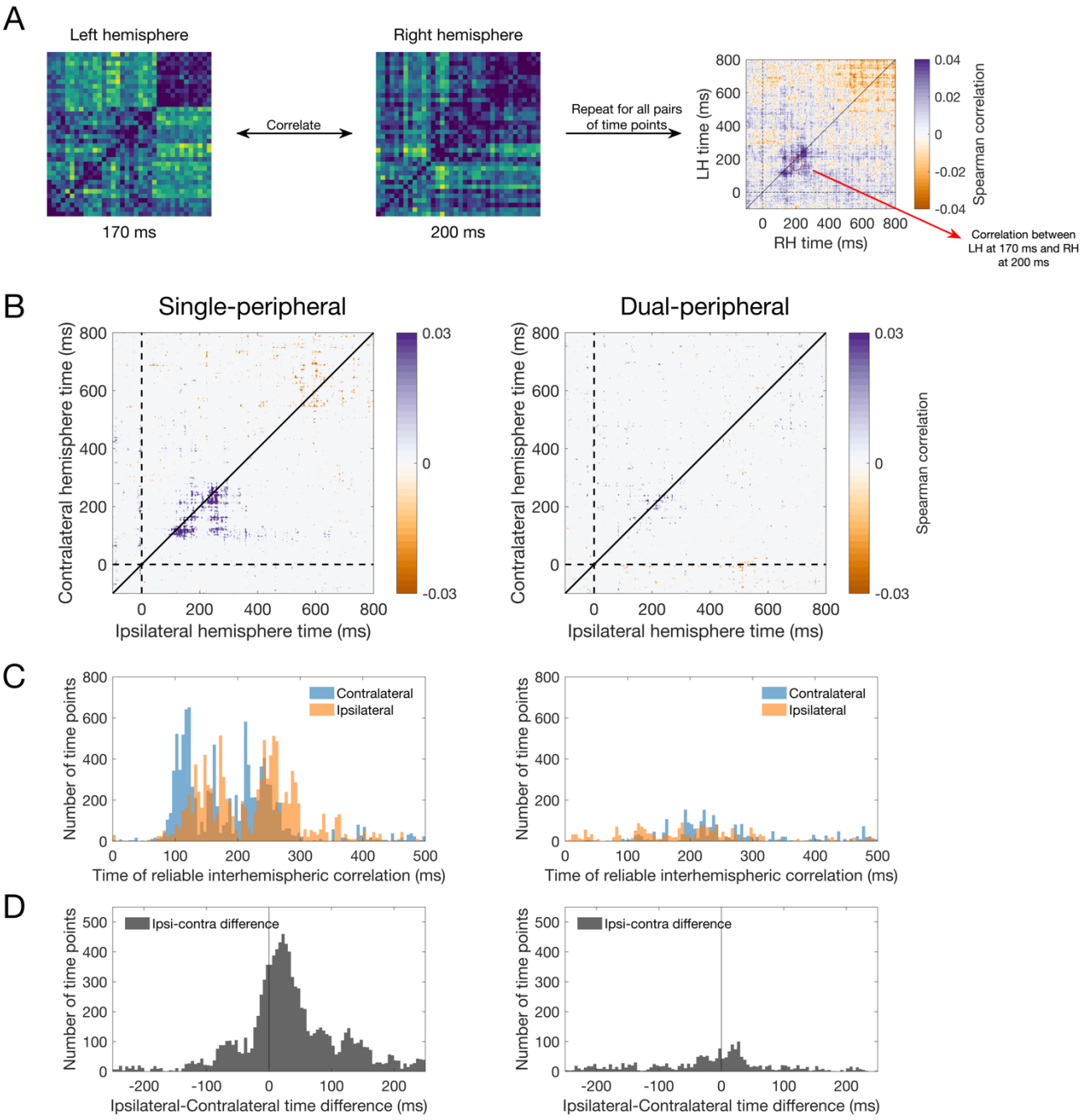

Note. A) Interhemispheric representational similarity approach for assessing shared information across the hemispheres. 36 × 36 stimulus neural representational dissimilarity matrices (an indexed by decoding accuracy) were correlated between the two hemispheres for every pair of time points using split-half cross-validation. This resulted in time × time hemispheric correlation matrices. If there was no delay between the hemispheres, the time generalisation plots would be symmetrical around the diagonal. B) Plots show mean time × time correlations for representational structure in the contralateral and ipsilateral hemispheres for the single-peripheral (left) and dual-peripheral (right) conditions. Plots are thresholded by points with evidence for cross-hemispheric correlations different from zero (BF>3). The highest correlations were observed for contralateral to ipsilateral delays in the peripheral conditions (i.e., below diagonal correlations). C) Time of reliable interhemispheric correlations. Histograms show number of reliable (BF>3) positive hemispheric

correlation time points as a function of contralateral and ipsilateral time. D) Hemispheric delay. Histograms show the temporal delays between ipsilateral and contralateral times for reliable (BF>3) times of positive interhemispheric correlation. Most reliable correlations occurred with a delay between 15-30ms from contralateral to ipsilateral hemispheres, for both the single-peripheral and dual-peripheral conditions.

Consistency within and across hemispheres

Next, we assessed the consistency in the structure of information within a hemisphere compared to information that is shared across hemispheres, to quantify unique versus shared hemispheric information. Within-hemisphere consistency was calculated as the correlation between RDMs from odd and even trial sequences for a given hemisphere. Across-hemisphere consistency was calculated as the correlation between RDMs from the left and right hemispheres for separate halves of the data (as in Figure 5). Mean within versus across hemisphere consistency for the single-peripheral condition is shown in Figure 6, collapsed across the left and right hemispheres to assess information within the contralateral and ipsilateral hemispheres relative to the shared information between them. Overall, there were higher correlations within the contralateral hemisphere than the shared ("across") hemisphere correlations, but no reliable differences between the ipsilateral consistency and the shared information. Together, these results suggest that the contralateral hemisphere contains unique information over and above that in the ipsilateral hemisphere, but that the information in the ipsilateral hemisphere is a subset of that from the contralateral hemisphere.

Figure 6. Consistency of information within versus across hemispheres.

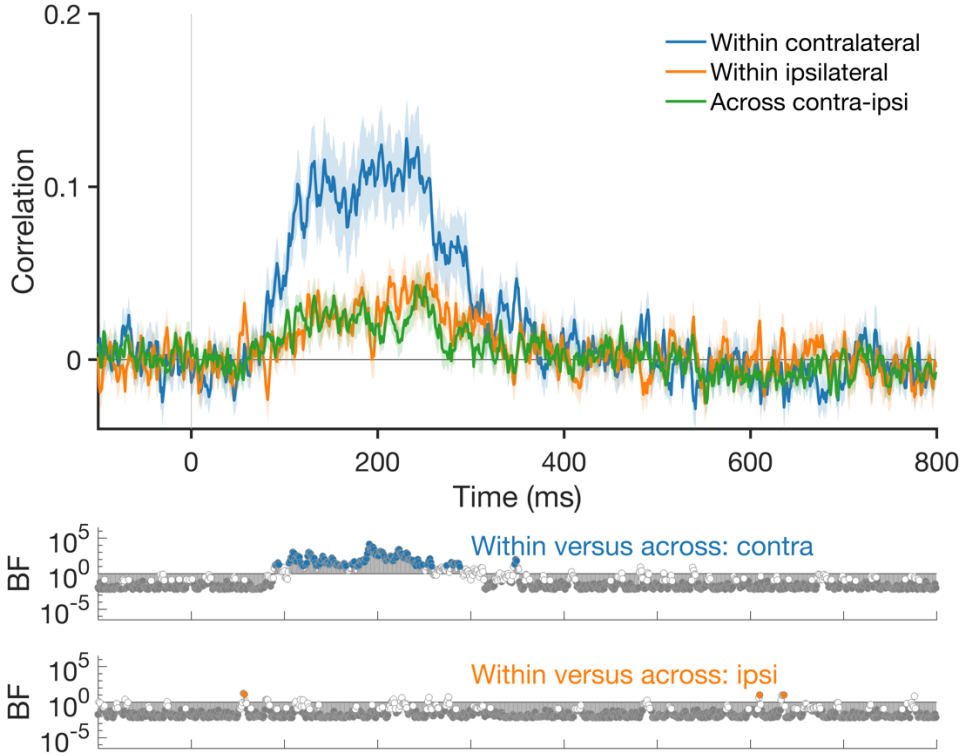

Note. Correlations between representational structure within and across hemispheres show unique information in the contralateral hemisphere above information that is shared with the ipsilateral hemisphere, but no unique information in the ipsilateral hemisphere. "Within" hemisphere consistency is calculated from a given hemisphere (contralateral/ipsilateral) using split-half Spearman correlation. "Across" hemisphere consistency is calculated as the correlation between the left and right hemispheres (as in Figure 5). Results are shown from the single-peripheral condition.

Behavioural relevance of neural representations

Having established that the representations of visual stimuli vary according to stimulus visual field and hemisphere, and that these representations are shared across hemispheres, we assessed their behavioural relevance to give insight into the content of the neural representations. We collated the perceptual dissimilarity of the 36 experimental stimuli obtained using online experiments. In each experiment, participants were presented with three stimuli simultaneously and asked to choose the odd-one-out according to two sets of instructions: "choose the one that looks different" (image task) or "choose the one that is conceptually different" (concept task) (Figure 7A). Stimulus dissimilarity was calculated as the proportion of odd-one-out choices for pairs of stimuli when they were presented together.

The behavioural results revealed that similarity judgements reflected both object category and meaning. To assess how the stimuli were clustered based on similarity judgements per task, we correlated the behavioural RDMs (Figure 7C) with models based on image/word category regardless of the object meaning (image model) and object type (concept model) (Figure 7B) using Spearman correlation. The image model correlated with behavioural judgements in the image task (r = .81, p < .001) and the concept task (r = .28, p < .001). Additionally, the concept model which distinguished the six object categories (bird, fish, tree, boat, face, tools), regardless of image/word status, also correlated with behaviour on the image task (r = .30, p < .001) and the concept task (r = .59, p < .001). Importantly, however, the image model had a higher correlation with the image similarity task than the concept similarity task (z = 20.96, p < .001) and the concept model had a lower correlation with behaviour on the image task than the concept task (z = -9.68, p < .001). Thus, although both the image and concept similarity tasks are correlated with both the image and concept model, there is a weighted asymmetry: images and words were chosen as more dissimilar in the image similarity task than the concept task because they look different despite sharing meaning and were intermixed and more related to the concept of the stimulus independent of perceptual format in the concept task. This asymmetry can be seen in the multi-dimensional visualisation of the results, where in the image task, words clustered separately to different image categories, but in the conceptual task, words clustered with their associated objects (Figure 7C-D).

Figure 7. Behavioural similarity tasks and results.

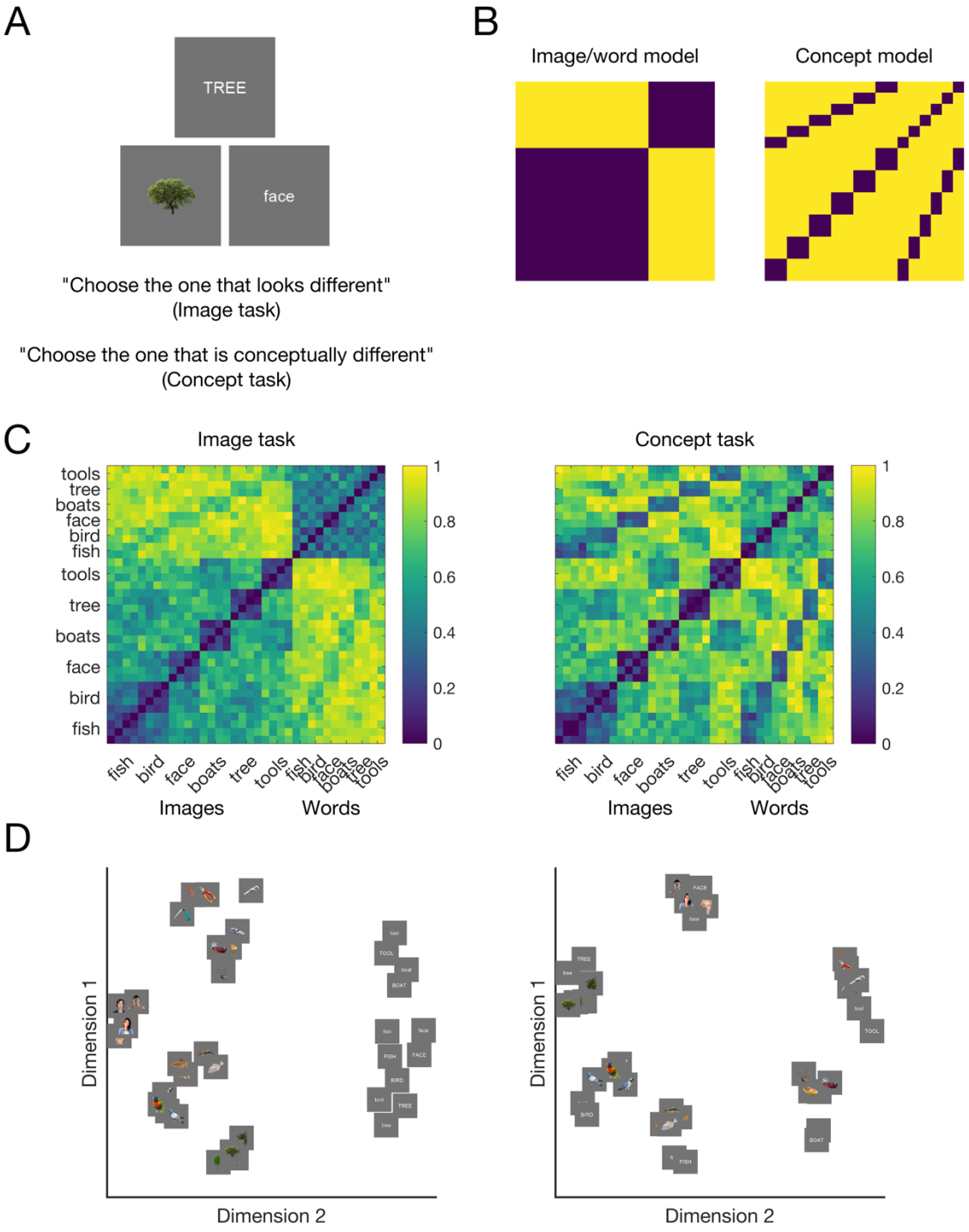

Note. (A) Behavioural task design. Three stimuli were presented simultaneously, and the task was to "choose the image that looks different" (image task) or "choose the image that is conceptually different" (concept task). (B) Stimulus models constructed for the 36 stimuli based on whether stimuli were images or words (left) or shared the same concepts (right). (C) Dissimilarity matrices based on the results from each behavioural task show relationships between the stimuli based on image/word classification (left; image similarity task) and object type (right; concept similarity task). D) Multi-dimensional scaling shows how stimuli clustered in the behavioural data. For the image similarity task (left), words formed a separate cluster from the images. For the conceptual similarity task (right), words and images of the same concept clustered together.

Using the behavioural models constructed from the two tasks, we assessed the behavioural relevance of the representations evoked in the contralateral and ipsilateral hemispheres. We used representational similarity analyses to compare the neural representations with behavioural models constructed from the image-similarity and concept-similarity versions of the odd-one-out task (Figure 7C). The logic of these analyses is shown in Figure 8A; neural RDMs at each time point were correlated with the image task RDM and concept task RDM to result in a time-varying neural-behaviour correlation for each task. This correlation was performed separately for the left and right hemispheres according to whether the stimuli were contralateral or ipsilateral. Figure 8B shows the mean neural-behaviour correlations for contralateral and ipsilateral conditions. We found that the behaviour reflected neural representations in the contralateral hemisphere (as indexed by above-zero correlations), and the neural-behaviour correlation was higher for the image task than the concept task. In contrast, the neural-behaviour relationship was similar for the image and concept tasks in the ipsilateral hemisphere, with greater statistical validity for the concept task. Together, these results indicate a fundamental difference in the types of information represented by the contralateral and ipsilateral hemispheres. Specifically, this suggests that information transfer from the contralateral to ipsilateral hemisphere might prioritise information that reflects object meaning; this likely includes certain visual features that are characteristic of object concepts, but not image statistics that are less relevant to object identity.

Figure 8. Neural-behaviour correlations for image and concept tasks.

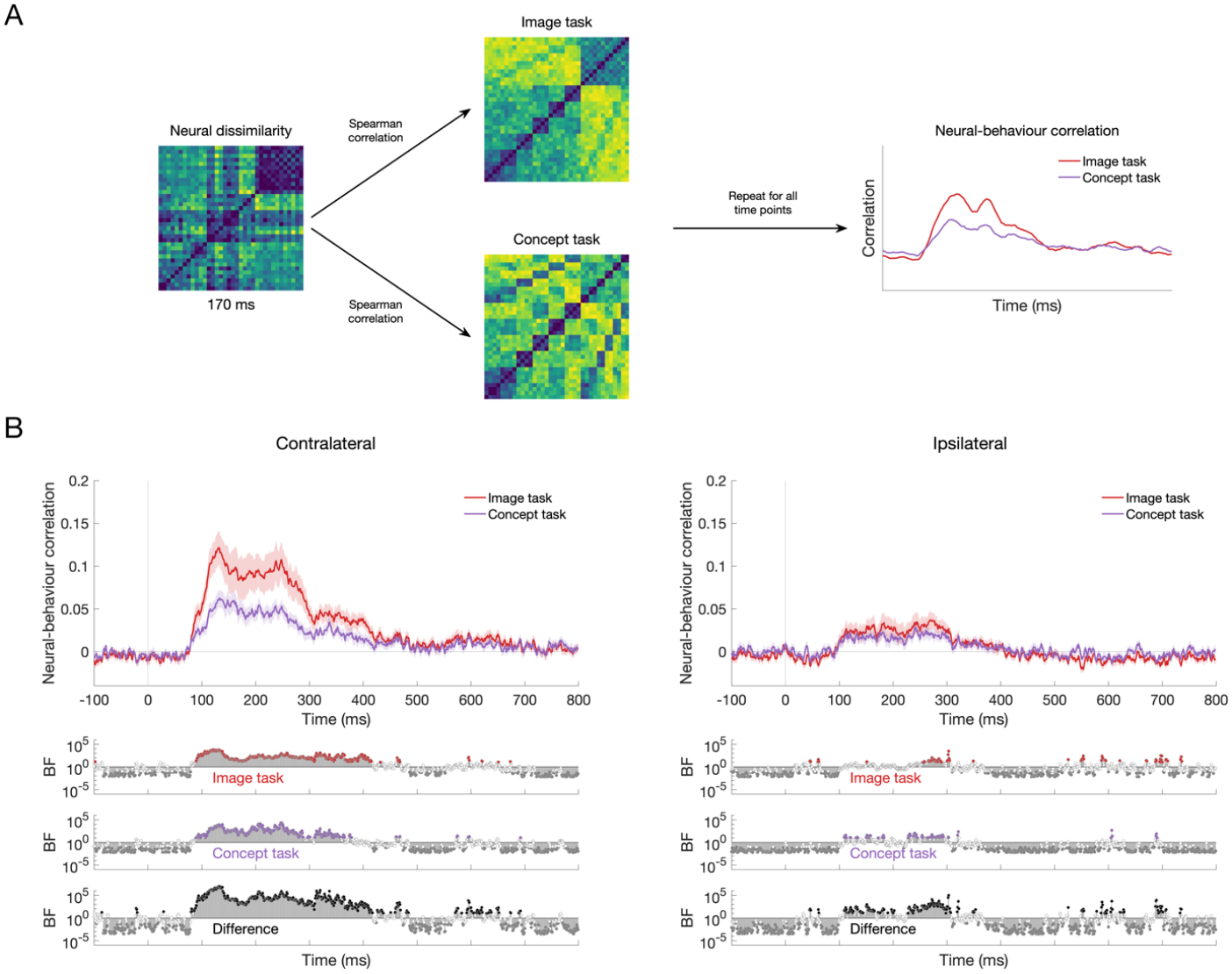

Note. A) Explanation of how neural-behaviour correlations were calculated. For each hemisphere and visual field condition, the neural dissimilarities across all 36 images were correlated with the behavioural dissimilarities for the image task and concept task, separately for each neural time point following image onset. The mean was subsequently calculated for the contralateral and ipsilateral conditions per behavioural task (example results plot shown). B). Neural-behaviour correlations across time for contralateral (left) and ipsilateral (right) stimulus presentations, collapsed across the left and right hemispheres. Behaviour from the image and concept tasks was reliably reflected in the neural signal in both hemispheres, though with less fidelity in the ipsilateral hemisphere particularly for the image task. Results are shown from the single-peripheral condition.

Discussion

In this study, we investigated the temporal dynamics of peripheral object processing within the left and right hemispheres. Across two different peripheral stimulus conditions, we found that image representations traverse the hemispheres across multiple stages of processing. Stimulus information was initially biased towards the contralateral hemisphere, but subsequent stages of processing showed robust neural responses in both hemispheres. Dynamics were different in the left and right hemispheres, regardless of whether the images were contralateral or ipsilateral. Specifically, the right hemisphere seemed to derive stimulus representations with higher fidelity than the left hemisphere, independent of visual field. Representational similarity analyses revealed that information is shared between the contralateral and ipsilateral hemispheres with a delay around 15-30ms. Finally, we found evidence that representations in both hemispheres correlate with behaviour on stimulus similarity tasks. While the contralateral hemisphere was more strongly correlated with image-related judgements than concept-related judgements, the ipsilateral hemisphere showed little difference in behavioural relevance for the two tasks. Together, these results suggest that hemispheric transfer prioritises object category information, which reflects both meaningful image features and object meaning, over image statistics that are not informative to meaning.

To our knowledge, this is the first study to assess representational dynamics in the left and right hemispheres in humans. We provide strong evidence of contralateral dominance of perceptual information in the visual system. This adds to previous work documenting contralateral dominance in the strength of neural activation (*10*–*12*) by showing that the contralateral hemisphere also represents visual *information* with higher fidelity than the ipsilateral hemisphere. Specifically, we found stronger and earlier representations for contralateral visual field relative to ipsilateral visual field stimuli. Yet, there were still relevant representations for ipsilateral stimuli, indexed by above chance decoding, indicating that information was transferred from the contralateral to ipsilateral hemispheres. This remained true even for the dual-peripheral condition: each hemisphere

contained information about the two stimuli that were presented simultaneously, regardless of whether they were in the contralateral or ipsilateral visual field. Our task was irrelevant with respect to the visual stimuli, so the sharing of information across hemispheres appears to be a fundamental feature of neural processing rather than a goal-driven process.

We found evidence for interference of information processing for two simultaneously presented peripheral images. Specifically, there was a reduction in information in the dual- relative to single-peripheral condition in both the contralateral and ipsilateral hemispheres, but only after initial stages of processing (later than 150ms). Thus, the first stages of processing seem to proceed unimpeded within retinotopic visual regions, but then hemispheric transfer influences the coding of visual information in mid- to high-level object coding regions. Indeed, previous EEG-fMRI work showed that high-level extrastriate regions respond to stimuli from both visual fields, whereas low-level extrastriate regions respond primarily to the contralateral hemifield (*23*). It should be noted that the simultaneous stimuli in the current study were presented in symmetrical positions relative to the vertical midline, and it could be that interference is particularly sensitive to this configuration. Nevertheless, the timing of the interference effects highlight some possibilities about the nature of different processing stages, namely regarding temporal multiplexing. A growing body of literature has revealed that multiple rapidly-presented images are represented simultaneously in the brain (*24–26*), yet the temporal resolution of processing decreases from low level to higher level regions in the visual hierarchy (*27*, *28*). In the context of peripheral image processing, a possibility is that early retinotopic brain regions quickly and process input from the contralateral hemifield serially, and then transfer information to higher regions within both hemispheres. These successive brain regions have longer temporal integration windows, which could plausibly lead to interference between different stimuli (e.g., masking), but would also enable integration when stimuli presented temporally or spatially adjacent are contextually related.

EEG is not known for its high spatial resolution, but we implemented several strategies to ensure the analyses were assessing distinct information from each hemisphere. First, we used clusters of electrodes that were spatially distinct, over the left and right occipitotemporal regions. Electrodes in these regions have previously been used to document hemispheric differences for face and word perception (*29–31*). Second, we performed a Laplacian transformation on the neural responses to highlight local patterns of activity, enhancing the spatial resolution of the signals (*32*). Indeed, the results indicate that there were distinct sources per hemisphere. The sensor searchlight analyses depict clear contralateral sources of information, with weaker ipsilateral clusters at later time points (see Supplementary Material). Finally, our time resolved decoding results show that the dynamics look distinct in the two hemispheres (e.g., with a later peak for ipsilateral stimuli). If there was only one neural source of information, we would expect an overall reduction for ipsilateral responses without a change in the timing.

In addition to varying dynamics for contralateral versus ipsilateral representations, the results of this study highlight differences between the left and right hemispheres of the brain. In particular, the left and right hemispheres seem to retain hemispheric-specific dynamics regardless of whether they are contralateral or ipsilateral, which is evidence that each hemisphere is specialised for certain types of information, and processing is distributed for these different processes. Furthermore, there was a consistent trend in which the right hemisphere had stronger representations than the left. Given the types of stimuli used in the current study, one could surmise that the hemispheric differences we observe are driven by the categories of words, which tend to be lateralised to the left hemisphere (*33*), and faces, which are lateralised to the right hemisphere (*34*). However, we find that even when separated by object category, there appears to be a consistent right hemispheric dominance in the strength of decoding (see Supplementary Material), which hints towards more general hemispheric processing differences, potentially centred around biases for specific visual features. It has been postulated that the two hemispheres contain distinct subsystems for abstract and specific visual object recognition (*35*, *36*), with the right hemisphere more effective for specific exemplar recognition, so one possibility is that

the focus on stimulus information in the current study inadvertently biases towards a right hemispheric advantage. However, it should be noted that the hemispheric neural-behavioural analyses showed stronger correlations for the image task in the right hemisphere, but there was no left advantage for the concept task, a task that likely required a more abstract recognition strategy.

Despite hemispheric differences, there was evidence of clear representational overlap between the hemispheres. Our results show the ipsilateral hemisphere represents stimulus information similarly but after a delay relative to the contralateral stimulus. Our estimates of the delay were on the order of 15-30ms. This again points to clear evidence of information transfer from one hemisphere to the other. More support for this transfer delay is evident from the delay of decoding onset for ipsilateral relative to contralateral stimuli (see Table 1). Beyond the timing differences, the similarity in the structure of stimulus representations between the hemispheres contralateral and ipsilateral to the experimental stimuli suggests an element of redundancy in the system. The ipsilateral hemisphere receives peripheral visual information indirectly, via the contralateral hemisphere, so shared or redundant information does not come as a surprise. Yet, this indirect transfer does not preclude different processes being carried out on inputs to the contralateral and ipsilateral hemispheres. We found the information within the hemisphere ipsilateral to the stimulus did not contain any unique information relative to the contralateral hemisphere, but rather the information was largely duplicated throughout the time course of processing. Importantly, however, the specific information that was transferred to the ipsilateral hemisphere was only a subset of that represented within the contralateral hemisphere. This raises the possibility that hemispheric transfer operates as a filtering mechanism, modulating neural activity to focus the most important types of information. Indeed, evidence suggests that cross-hemispheric neurons are mainly excitatory but they target both excitatory and inhibitory neurons (*37*), which seems a plausible route for information pruning. So, despite the apparent redundancy across the hemispheres, perhaps the ipsilateral hemisphere plays an important role in being able to process only the most relevant information.

Our analyses into the behavioural relevance of the neural representations supports this "filtering via hemispheric transfer" theory. The contralateral hemisphere was biased towards perceptual over conceptual judgements, with behavioural responses on the image task accounting for more variance within the neural signal than responses on the concept task. Yet, in the ipsilateral hemisphere there was little difference between the behavioural relevance for perceptual and conceptual judgements. Behavioural responses in the image task and concept task, while separable, were highly correlated, so we would not expect them to necessarily dissociate. We suggest that similar neural-behavioural correlations for both tasks in the ipsilateral hemisphere probably reflects judgements that are common between the two tasks, which seem to be object-category focused. In contrast, the types of information that were lost to hemispheric transfer mainly related to perceptual judgements, likely related to image statistics. These findings indicate that hemispheric transfer might prioritise information relating to object identity; this includes object meaning as well as image features that are characteristic of object identity (e.g., trees tend to be green). While there are still many open questions about the nature of hemispheric transfer, we think this is a promising line of research and future work can try to disentangle the specific types of information that are prioritised for transfer across the hemispheres.

Materials and Methods

All code, stimuli and behavioural data are available at https://github.com/amandakrobinson/hemifield-eeg and EEG data are available at https://openneuro.org/datasets/ds005087.

Participants

Participants were 20 adults recruited from the University of Sydney (15 females, median age 22 years) in return for payment or course credit. The study was approved by the University of Sydney ethics committee and informed consent was obtained from all participants. Edinburgh handedness scores indicated 17 participants were right-handed, 1 was left-handed and 2 were ambidextrous. The same trend in results was seen if only right-handed

individuals were analysed (see Supplementary Material). All participants reported normal or corrected-to-normal vision.

Stimuli and Design

Participants viewed images that appeared centrally or to the left or right of fixation on a 1920 × 1080 resolution ASUS VG236 monitor while their neural activity was measured with EEG. There were 36 stimuli: four different image exemplars of 6 basic objects: fish, bird, face, boat, tree and tool; and word labels for the same 6 objects in lower and upper case (Figure 1A). Half the trials were words and half were objects. Stimuli were presented at approximately 3.24 × 3.24 degrees of visual angle, and at an eccentricity of 3.24 degrees to the centre of the object. All stimuli were presented using Psychopy (*38*). We intended to present the words in italics as well as original typeface but an unforeseen issue with the PsychoPy presentation meant the italics were not applied, so each specific word stimulus was presented double the number of times compared with each object (but only half of these were analysed, see below).

There were three types of experimental sequences: central, single-peripheral and dual-peripheral (Figure 1B). These sequences were interleaved throughout the experimental session. Here, we focus only on the peripheral and dual-peripheral sequences as these inputs are projected to a single hemisphere in a bottom-up fashion. In each sequence, there were 192 trials. Each trial was presented for 100ms with a gap of 100ms between trials (5 Hz presentation). In the single-peripheral condition, stimuli were presented half to the left and half to the right of fixation equiprobably and in random order, with only one stimulus presented at a time. Each sequence consisted of 4 repeats per object stimulus (2 on the left and 2 on the right) and 8 repeats per word stimulus (4 left; 4 right). In the dual-peripheral condition, every trial consisted of one stimulus to the left and one to right visual field simultaneously. There were 96 images and 96 words on each side in random combinations. Within each sequence, trials were presented in random order. Across the experiment, there were 24 single-peripheral and 12 dual-peripheral sequences, which, in total, contained the same number of stimulus repeats per visual field. In sum, there were

48 repeats of each of the 24 image stimuli and 96 repeats of each of the 12 word stimuli in each hemifield for each condition. To maintain equal trial numbers per class, only 48 repeats for the word stimuli were analysed, randomly selected.

During the experimental session, participants were asked to monitor the three dots (central fixation, left and right) marking the possible stimulus locations and detect when one turned red (Figure 1B) and indicate detection by button press. Participants were asked to maintain fixation on the central dot. This task was designed to be orthogonal and irrelevant to the stimuli, but ensured that participants maintained attention across the whole visual field throughout the experiment, regardless of stimulus presentation condition.

EEG recording and preprocessing

EEG data were continuously recorded from 64 electrodes arranged in the international 10–20 system for electrode placement (*39*) using a BrainProducts ActiChamp system, digitized at a 1000Hz sample rate. Scalp electrodes were referenced to Cz during recording. The EEGLAB toolbox (*40*) was used to preprocess the data offline. First, we interpolated electrodes that exceed 5 standard deviations of kurtosis, then a common average reference was applied. We filtered the data using a Hamming windowed sinc FIR filter with highpass of 0.1Hz and lowpass of 100Hz as in our previous work (*24*, *26*). Downsampling was not applied, so the temporal resolution of the data was 1ms. Epochs were created for each stimulus presentation ranging from -100 to 800ms relative to stimulus onset. Finally, we used the CSD toolbox (*41*) to perform a Laplacian transformation (*32*) which calculates the second spatial derivative of the scalp potentials. This transformation enhances the spatial resolution of the EEG signal at the scalp, in our case ensuring greater distinction between left and right hemispheric responses.

Neural decoding

To investigate the neural representations of lateralised stimuli in the two hemispheres, we used multivariate pattern analyses to assess stimulus-specific representations per hemifield

(left/right), hemisphere (left/right) and presentation condition (single-/dual-peripheral). Given that EEG responses are typically stronger for contralateral stimuli (*12*), we expected that stimuli would also be represented with higher fidelity in the contralateral hemisphere than the ipsilateral hemisphere, and potentially represented with different dynamics. Further, we were interested in how conflicting information to the hemispheres (as in the dual-peripheral condition) influenced the neural representations relative to the single-peripheral condition.

EEG data were analysed using time-resolved classification methods and implemented using the CoSMoMVPA toolbox (*42*). Decoding was performed separately for the left and right hemispheres using clusters of six occipito-temporal electrodes (Figure 1C). The electrodes chosen were O1, PO3, PO7, P3, P5 and P7 for the left cluster, and O2, PO4, PO8, P4, P6 and P8 for the right cluster. These clusters encompass similar electrodes to previous work investigating lateralised responses (*29–31*), but containing sufficient electrodes to allow for pattern analysis. Decoding was performed separately for each participant, for each presentation condition (single/dual × left/right hemifield) and for each single time point in the epoch (1 ms time resolution). Data were pooled across the 6 EEG sensors in each cluster, and we tested the ability of a linear discriminant analysis (LDA) classifier to discriminate between the patterns of neural responses associated with each stimulus. A 12-fold cross-validation procedure was used, with each fold containing independent trial sequences. All pairs of combinations for the 36 stimuli (e.g., face1 vs tree2, word-tool1 vs fish4) were decoded, resulting in 630 unique contrasts across time per condition per participant. Classifier accuracy was calculated as the proportion of correct classifier predictions across all folds, and the group mean was calculated per condition. All decoding contrasts were pairwise, so chance performance was 0.5. Accuracy of classifier predictions reflected the information in the neural signal, where above-chance classification accuracy (>0.5) indicated that the hemisphere contained information about the stimuli.

Behavioural similarity task

We were also interested in how the neural responses within each hemisphere related to behavioural judgements for the same stimuli. In two online experiments (*43*), conducted independently of the EEG acquisition, new groups of participants rated the similarity between the experimental stimuli using a triplet odd-one-out task (*44*, *45*) with the 36 experimental stimuli.

Participants were undergraduate students from the University of Sydney who participated in return for course credit. The experiments were programmed in jsPsych (*46*) and hosted on Pavlovia (*38*). In each experiment, there was a separate set of instructions: "choose the one that looks different" (N = 21), or "choose the one that is conceptually different" (N = 21). On each trial, three experimental stimuli were presented simultaneously, and participants were asked to choose the odd one out by clicking on the stimulus (Figure 2A). There were 400 trials in the experiment, and stimulus combinations were randomly chosen.

Behavioural responses were used to construct representational dissimilarity matrices for each task. For each trial, we calculated dissimilarity across the pairs of stimuli (3 pairs for the 3 distinct stimuli). The chosen odd-one-out stimulus was coded as dissimilar from each of the other two stimuli (value of 1), and the two other stimuli were coded as similar (value of 0). Across all trials of all participants, the dissimilarity of each stimulus pair (e.g., face1 vs word-tree2) was calculated as the mean response for all trials in which those two stimuli were presented together, a measure of their relative similarity to each other compared with the other stimuli in the set.

Representational similarity analyses

To investigate the relationship in the structure of stimulus representations between the two hemispheres, we used representational similarity analyses (RSA) (*22*). RSA allowed a comparison between hemispheres which was abstracted away from specific neural activity patterns, and rather focused on the relationships between stimulus representations. In this case, RSA allowed hemispheric-specific representations to be compared with representations of the other hemisphere in the single- and dual-peripheral conditions. In a

subsequent set of analyses, we used RSA to compare representations within each hemisphere with behavioural judgements, to assess the content of information within each hemisphere.

Using the neural and behavioural results, we constructed representational dissimilarity matrices (RDMs), which quantified the similarity between each stimulus (e.g., Figure 5A). Each of these RDM models was a 36 × 36 matrix of dissimilarity for each of the 36 stimuli with each other stimulus, using the relevant neural or behavioural measure. The RDMs were symmetrical across the diagonal, with 630 unique values. Neural RDMs used decoding accuracy for each pair of stimuli at each time point (1 ms temporal resolution). Separate 36 × 36 stimulus RDMs were constructed for each hemisphere, time point and participant, where each cell contained the mean decoding accuracy between two stimuli. The behavioural RDMs were based on the group mean dissimilarity scores from the two behavioural experiments. We also constructed two additional stimulus models based on the stimulus category (image/word) and concept (e.g., tree, tool, face).

Using RSA, we investigated how representations varied across the hemispheres. First, we correlated the left and right hemisphere RDMs using Spearman correlation to assess similarity of the lower diagonals of the RDMs (i.e., the unique pairwise values), for every pair of time points. This allowed us to assess how representations were similar across the hemispheres, and whether this similarity was dependent on transfer delays. Finally, we correlated the neural models across time with each behavioural model to assess how neural information might inform overall perception. Correlations were performed for each EEG participant separately and the mean was calculated across the group.

For any analyses comparing hemispheres, we used a split-half comparison method to reduce spurious correlations due to correlated noise. Specifically, we constructed two RDMs per condition, based on odd or even sequences (i.e., using 6-fold cross-validation to decode stimulus pairs). We then assessed similarity in neural RDMs across hemispheres by using different sequences; for example, comparing the left hemisphere RDM from odd

sequences with the right hemisphere RDM from even sequences and vice versa, then taking the mean.

Statistical testing

To assess neural representations within the hemispheres, we used Bayesian statistics to determine the evidence for the alternative relative to the null hypotheses (*47–51*). For decoding analyses, the alternative hypothesis of above-chance (50%) decoding was tested. For correlation analyses, the alternative hypotheses of above- and below- zero correlations were tested. We used the 'BayesFactor' package in R (*52*). Bayes Factors were calculated using a JZS prior, centred around chance decoding of 50% (*50*) with default scale factor of 0.707, meaning that for the alternative hypotheses of above- and below- chance decoding, we expected to see 50% of parameter values falling within -.707 and .707 standard deviations from chance (*49*, *50*, *53*, *54*). A null interval was specified as a range of effect sizes between -0.5 to 0.5 (*55*).

A Bayes Factor (BF) is the probability of the data under the alternative hypothesis relative to the null hypothesis. We consider BF > 3 as evidence for the alternative hypothesis (above-chance decoding and reliable correlations). To calculate the onset of effects, we used a conservative estimate of the first time that there was sustained evidence for 10 ms (ten consecutive time points with BF > 10). We interpreted BF < 1/3 as evidence in favour of the null hypothesis (*49*, *56*).

References

1. M. S. Gazzaniga, Organization of the Human Brain. *Science* **245**, 947–952 (1989).
2. G. R. Mangun, S. J. Luck, R. Plager, W. Loftus, S. A. Hillyard, T. Handy, V. P. Clark, M. S. Gazzaniga, Monitoring the visual world: hemispheric asymmetries and subcortical processes in attention. *J Cogn Neurosci* **6**, 267–275 (1994).
3. A. Belger, M. T. Banich, Costs and benefits of integrating information between the cerebral hemispheres: A computational perspective. *Neuropsychology* **12**, 380–398 (1998).

4. K. Yoshizaki, D. H. Weissman, M. T. Banich, A hemispheric division of labor aids mental rotation. *Neuropsychology* **21**, 326–336 (2007).

5. G. M. Innocenti, "General Organization of Callosal Connections in the Cerebral Cortex" in *Sensory-Motor Areas and Aspects of Cortical Connectivity*, E. G. Jones, A. Peters, Eds. (Springer US, Boston, MA, 1986; https://doi.org/10.1007/978-1-4613-2149-1_9), pp. 291–353.

6. G. F. Poggio, T. Poggio, The Analysis of Stereopsis. *Annual Review of Neuroscience* **7**, 379–412 (1984).

7. N. van Meer, A. C. Houtman, P. Van Schuerbeek, T. Vanderhasselt, C. Milleret, M. P. ten Tusscher, Interhemispheric Connections between the Primary Visual Cortical Areas via the Anterior Commissure in Human Callosal Agenesis. *Front. Syst. Neurosci.* **10** (2016).

8. J. J. DiCarlo, D. Zoccolan, N. C. Rust, How does the brain solve visual object recognition? *Neuron* **73**, 415–434 (2012).

9. M. Riesenhuber, T. Poggio, Models of object recognition. *Nature neuroscience* **3 Suppl**, 1199–204 (2000).

10. C. R. Lines, M. D. Rugg, A. D. Milner, The effect of stimulus intensity on visual evoked potential estimates of interhemispheric transmission time. *Exp Brain Res* **57**, 89–98 (1984).

11. G. R. Mangun, Neural mechanisms of visual selective attention. *Psychophysiology* **32**, 4–18 (1995).

12. C. D. Saron, R. J. Davidson, Visual evoked potential measures of interhemispheric transfer time in humans. *Behavioral Neuroscience* **103**, 1115–1138 (1989).

13. F. Aboitiz, A. B. Scheibel, R. S. Fisher, E. Zaidel, Fiber composition of the human corpus callosum. *Brain Research* **598**, 143–153 (1992).

14. J. L. Andreassi, H. Okamura, M. Stern, Hemispheric Asymmetries in the Visual Cortical Evoked Potential as a Function of Stimulus Location. *Psychophysiology* **12**, 541–546 (1975).

15. R. Srebro, The topography of scalp potentials evoked by pattern pulse stimuli. *Vision Research* **27**, 901–914 (1987).

16. M. N. Hebart, C. I. Baker, Deconstructing multivariate decoding for the study of brain function. *NeuroImage* **180**, 4–18 (2018).

17. A. K. Robinson, G. L. Quek, T. A. Carlson, Visual Representations: Insights from Neural Decoding. *Annual Review of Vision Science* **9**, 313–335 (2023).

18. T. A. Carlson, H. Hogendoorn, R. Kanai, J. Mesik, J. Turret, High temporal resolution decoding of object position and category. *Journal of Vision* **11**, 9–9 (2011).

19. R. M. Cichy, D. Pantazis, A. Oliva, Resolving human object recognition in space and time. *Nature Neuroscience* **17**, 455–462 (2014).

20. A. K. Robinson, P. Venkatesh, M. J. Boring, M. J. Tarr, P. Grover, M. Behrmann, Very high density EEG elucidates spatiotemporal aspects of early visual processing. *Scientific Reports* **7**, 1–11 (2017).

21. T. Grootswagers, H. McKay, M. Varlet, Unique contributions of perceptual and conceptual humanness to object representations in the human brain. *NeuroImage* **257**, 119350 (2022).

22. N. Kriegeskorte, M. Mur, P. a. Bandettini, Representational similarity analysis - connecting the branches of systems neuroscience. *Frontiers in systems neuroscience* **2**, 4–4 (2008).

23. Z. Liu, N. Zhang, W. Chen, B. He, Mapping the bilateral visual integration by EEG and fMRI. *NeuroImage* **46**, 989–997 (2009).

24. T. Grootswagers, A. K. Robinson, T. A. Carlson, The representational dynamics of visual objects in rapid serial visual processing streams. *NeuroImage* **188**, gro (2019).

25. J.-R. King, V. Wyart, The Human Brain Encodes a Chronicle of Visual Events at Each Instant of Time Through the Multiplexing of Traveling Waves. *J. Neurosci.* **41**, 7224–7233 (2021).

26. A. K. Robinson, T. Grootswagers, T. A. Carlson, The influence of image masking on object representations during rapid serial visual presentation. *NeuroImage* **197**, 224–231 (2019).

27. B. Gauthier, E. Eger, G. Hesselmann, A.-L. Giraud, A. Kleinschmidt, Temporal Tuning Properties along the Human Ventral Visual Stream. *J. Neurosci.* **32**, 14433–14441 (2012).

28. T. J. McKeeff, D. A. Remus, F. Tong, Temporal Limitations in Object Processing Across the Human Ventral Visual Pathway. *Journal of Neurophysiology* **98**, 382–393 (2007).

29. S. Bentin, T. Allison, A. Puce, E. Perez, G. Mccarthy, Electrophysiological Studies of Face Perception in Humans. *Journal of cognitive neuroscience* **8**, 551–565 (1996).

30. A. K. Robinson, D. C. Plaut, M. Behrmann, Word and face processing engage overlapping distributed networks: Evidence from RSVP and EEG investigations. *Journal of Experimental Psychology: General* **146**, 943–961 (2017).

31. B. Rossion, C. A. Joyce, G. W. Cottrell, M. J. Tarr, Early lateralization and orientation tuning for face , word , and object processing in the visual cortex. **20**, 1609–1624 (2003).

32. F. Perrin, J. Pernier, O. Bertrand, J. F. Echallier, Spherical splines for scalp potential and current density mapping. *Electroencephalography and Clinical Neurophysiology* **72**, 184–187 (1989).

33. L. Cohen, S. Dehaene, L. Naccache, S. Lehéricy, G. Dehaene-Lambertz, M. A. Hénaff, F. Michel, The visual word form area: Spatial and temporal characterization of an initial stage of reading in normal subjects and posterior split-brain patients. *Brain* **123**, 291–307 (2000).

34. N. Kanwisher, J. Mcdermott, M. M. Chun, The Fusiform Face Area : A Module in Human Extrastriate Cortex Specialized for Face Perception. *Journal of Neuroscience* **17**, 4302–4311 (1997).

35. E. D. Burgund, C. J. Marsolek, Letter-case-specific priming in the right cerebral hemisphere with a form-specific perceptual identification task. *Brain and Cognition* **35**, 239–258 (1997).

36. C. J. Marsolek, Dissociable Neural Subsystems Underlie Abstract and Specific Object Recognition. *Psychol Sci* **10**, 111–118 (1999).

37. S. Ocklenburg, Z. V. Guo, Cross-hemispheric communication: Insights on lateralized brain functions. *Neuron* **0** (2024).

38. J. Peirce, J. R. Gray, S. Simpson, M. MacAskill, R. Höchenberger, H. Sogo, E. Kastman, J. K. Lindeløv, PsychoPy2: Experiments in behavior made easy. *Behav Res Methods* **51**, 195–203 (2019).

39. R. Oostenveld, P. Praamstra, The five percent electrode system for high-resolution EEG and ERP measurements. *Clinical Neurophysiology* **112**, 713–719 (2001).

40. A. Delorme, S. Makeig, EEGLAB: An open source toolbox for analysis of single-trial EEG dynamics including independent component analysis. *Journal of Neuroscience Methods* **134**, 9–21 (2004).

41. J. Kayser, C. E. Tenke, Principal components analysis of Laplacian waveforms as a generic method for identifying ERP generator patterns: I. Evaluation with auditory oddball tasks. *Clinical Neurophysiology* **117**, 348–368 (2006).

42. N. N. Oosterhof, A. C. Connolly, J. V. Haxby, CoSMoMVPA: Multi-Modal Multivariate Pattern Analysis of Neuroimaging Data in Matlab/GNU Octave. *Front. Neuroinform.* **10** (2016).

43. T. Grootswagers, A primer on running human behavioural experiments online. *Behav Res Methods* **52**, 2283–2286 (2020).

44. T. Grootswagers, A. K. Robinson, S. M. Shatek, T. A. Carlson, Mapping the dynamics of visual feature coding: Insights into perception and integration. *PLOS Computational Biology* **20**, e1011760 (2024).

45. M. N. Hebart, C. Y. Zheng, F. Pereira, C. I. Baker, Revealing the multidimensional mental representations of natural objects underlying human similarity judgements. *Nat Hum Behav* **4**, 1173–1185 (2020).

46. J. R. de Leeuw, jsPsych: a JavaScript library for creating behavioral experiments in a Web browser. *Behav Res Methods* **47**, 1–12 (2015).

47. Z. Dienes, Bayesian Versus Orthodox Statistics: Which Side Are You On? *Perspectives on Psychological Science* **6**, 274–290 (2011).

48. Z. Dienes, How Bayes factors change scientific practice. *Journal of Mathematical Psychology* **72**, 78–89 (2016).

49. H. Jeffreys, *Theory of Probability* (Oxford University Press, Oxford, Third., 1961).

50. J. N. Rouder, P. L. Speckman, D. Sun, R. D. Morey, G. Iverson, Bayesian t tests for accepting and rejecting the null hypothesis. *Psychon Bull Rev* **16**, 225–237 (2009).

51. E. Wagenmakers, A practical solution to the pervasive problems of p values. *Psychonomic Bulletin and Review* **14**, 779–804 (2007).

52. R. D. Morey, J. N. Rouder, T. Jamil, S. Urbanek, K. Forner, A. Ly, Package "BayesFactor" (2018). https://cran.r-project.org/web/packages/BayesFactor/BayesFactor.pdf.

53. R. Wetzels, E.-J. Wagenmakers, A default Bayesian hypothesis test for correlations and partial correlations. *Psychon Bull Rev* **19**, 1057–1064 (2012).

54. A. Zellner, A. Siow, Posterior odds ratios for selected regression hypotheses. *Trabajos de Estadistica Y de Investigacion Operativa* **31**, 585–603 (1980).

55. L. Teichmann, D. Moerel, C. Baker, T. Grootswagers, "An empirically-driven guide on using Bayes Factors for M/EEG decoding" (2021); https://doi.org/10.1101/2021.06.23.449663.

56. R. Wetzels, D. Matzke, M. D. Lee, J. N. Rouder, G. J. Iverson, E. J. Wagenmakers, Statistical evidence in experimental psychology: An empirical comparison using 855 t tests. *Perspectives on Psychological Science* **6**, 291–298 (2011).

Acknowledgments

We would like to acknowledge the University of Sydney HPC service for providing High Performance Computing resources.

Funding

Australian Research Council Discovery Early Career Researcher Award DE200101159 (AKR)

Australian Research Council Discovery Early Career Researcher Award DE230100380 (TG)

Australian Research Council Discovery Project DP160101300 (TAC)

Australian Research Council Discovery Project DP200101787 (TAC)

National Science Foundation grant BCS2123069 (MB).

National Eye Institute, NIH P30 CORE award EY08098 (MB)

Unrestricted supporting funds from The Research to Prevent Blindness Inc, NY, and the Eye & Ear Foundation of Pittsburgh (MB).